



Combined Geometric and Neural Network Approach to Generic Fault Diagnosis in Satellite Actuators and Sensors

Baldi, P.; Blanke, Mogens; Castaldi, P.; Mimmo, N.; Simani, S.

Published in:
IFAC-PapersOnLine

Link to article, DOI:
[10.1016/j.ifacol.2016.09.074](https://doi.org/10.1016/j.ifacol.2016.09.074)

Publication date:
2016

Document Version
Peer reviewed version

[Link back to DTU Orbit](#)

Citation (APA):
Baldi, P., Blanke, M., Castaldi, P., Mimmo, N., & Simani, S. (2016). Combined Geometric and Neural Network Approach to Generic Fault Diagnosis in Satellite Actuators and Sensors. *IFAC-PapersOnLine*, 49(17), 432–437. <https://doi.org/10.1016/j.ifacol.2016.09.074>

General rights

Copyright and moral rights for the publications made accessible in the public portal are retained by the authors and/or other copyright owners and it is a condition of accessing publications that users recognise and abide by the legal requirements associated with these rights.

- Users may download and print one copy of any publication from the public portal for the purpose of private study or research.
- You may not further distribute the material or use it for any profit-making activity or commercial gain
- You may freely distribute the URL identifying the publication in the public portal

If you believe that this document breaches copyright please contact us providing details, and we will remove access to the work immediately and investigate your claim.

Combined Geometric and Neural Network Approach to Generic Fault Diagnosis in Satellite Actuators and Sensors

P. Baldi^{*,1} M. Blanke^{**} P. Castaldi^{*} N. Mimmo^{*}
S. Simani^{***}

^{*} *Dipartimento di Ingegneria dell'Energia Elettrica e dell'Informazione, Università di Bologna, Facoltà di Ingegneria Aerospaziale. 47100 Forlì(FC), Italy. (e-mail: pietro.baldi2@unibo.it).*

^{**} *Department of Electrical Engineering, Technical University of Denmark, 2800 Kgs. Lyngby, Denmark. (e-mail: mb@elektro.dtu.dk)*

^{***} *Dipartimento di Ingegneria, Università di Ferrara. 44123 Ferrara (FE), Italy. (e-mail: silvio.simani@unife.it).*

Abstract: This paper presents a novel scheme for diagnosis of faults affecting the sensors measuring the satellite attitude, body angular velocity and flywheel spin rates as well as defects related to the control torques provided by satellite reaction wheels. A nonlinear geometric design is used to avoid that aerodynamic disturbance torques have unwanted influence on the residuals exploited for fault detection and isolation. Radial basis function neural networks are used to obtain fault estimation filters that do not need a priori information about the fault internal models. Simulation results are based on a detailed nonlinear satellite model with embedded disturbance description. The results document the efficacy of the proposed diagnosis scheme.

Keywords: Fault diagnosis, geometric approaches, neural networks, actuators, sensors, satellite control applications.

1. INTRODUCTION

The increasing operational requirements for onboard autonomy in satellite control systems require structural methods that support the design of complete and reliable Fault Detection and Diagnosis (FDD) systems providing fundamental information about the system health status jointly with accurate fault estimates. Significant research in FDD has been done in the last decades (Isermann (2011); Blanke et al. (2016)). Numerous model-based methods have been proposed for fault diagnosis (Chen-Patton (1999); Ding (2013)) and for the diagnosis in nonlinear systems (Bokor-Szabó (2009)). In particular, a solution to the Fault Detection and Isolation (FDI) problem for nonlinear systems is presented in De Persis-Isidori (2001) through the NonLinear Geometric Approach (NLGA). This paper presents a novel diagnosis scheme to assess the health condition and proper functioning of essential sensors and actuators of a satellite Attitude Determination and Control Systems (ADCSs). This work is a substantial improvement of a previous work of the same authors (Baldi et al. (2015)), which considered only faults affecting the attitude control torques and flywheel spin rate sensors. In contrast, this paper considers also possible faults affecting the satellite attitude and angular velocity sensors. The procedure for actuator and sensor fault modelling presented in Mattone-De Luca (2006) is exploited to define a nonlinear model affine in all the actuator and sensor fault inputs and suitable for the NLGA application.

The performances of the proposed FDD system have been evaluated when applied to a detailed nonlinear satellite simulator. In particular, the exogenous disturbance terms represented by the aerodynamic and gravitational disturbance torques are considered. As the gravitational disturbance model is almost perfectly known, the FDD robustness is achieved by exploiting an *explicit disturbance decoupling* based on the NLGA, applied only to the aerodynamic force term (Baldi et al. (2015)). In fact, this term represents the main source of uncertainty in the satellite dynamic model, mainly due to the lack of knowledge of the accurate values of air density and satellite drag coefficient. The scalar residual filters composing the FDI module of the model-based FDD system are designed via the NLGA to obtain diagnostic signals that are independent of the knowledge of the aerodynamic disturbance parameters. The fault isolation is achieved by means of a residual cross-check and a proper decision logic, assuming a single fault occurring at any time. The adaptive filters of the Fault Estimation (FE) module are designed via Radial Basis Function Neural Networks (RBF NN)s (Chen-Chen (1995); Castaldi et al. (2014)) and activated once a fault has been correctly detected and isolated.

The use of a RBF NN allows to design *generalised fault estimation filters* that do not need a priori information about the type of the occurred fault and that are capable of accurately estimating a generic fault without needing to define any specific fault internal model. Moreover, the NLGA allows to obtain a precise FDI and accurate fault estimates, independent of the knowledge of the aerodynamic

¹ Corresponding author.

disturbance parameters, and thus without any isolation and estimation errors due to parameter uncertainties. Simulation results are given in case of both actuator and sensor faults, validating the ability of the proposed scheme to deal with faults of different types, provide a precise fault detection, isolation and accurate fault estimates.

2. SATELLITE AND ACTUATOR MODELS

The satellite is considered as a rigid body, whose attitude is represented by using the quaternion notation. The satellite mathematical model is given by the dynamic and kinematic equations of (1) and (2) (Wie (2008)):

$$\begin{aligned}\dot{\boldsymbol{\omega}} &= -\mathbf{I}_s^{-1}\mathbf{S}(\boldsymbol{\omega})(\mathbf{I}_s\boldsymbol{\omega} + \mathbf{T}_{rw}\mathbf{h}_{rw}) + \mathbf{I}_s^{-1}(\mathbf{T}_{rw}\mathbf{M} + \mathbf{M}_{gg} + \mathbf{M}_{aero}) \quad (1) \\ \dot{\mathbf{q}} &= \frac{1}{2}\boldsymbol{\Omega}\mathbf{q} \quad (2)\end{aligned}$$

with the skew-symmetric matrices

$$\mathbf{S}(\boldsymbol{\omega}) = \begin{bmatrix} 0 & -\omega_3 & \omega_2 \\ \omega_3 & 0 & -\omega_1 \\ -\omega_2 & \omega_1 & 0 \end{bmatrix}, \boldsymbol{\Omega}(\boldsymbol{\omega}) = \begin{bmatrix} 0 & \omega_3 & -\omega_2 & \omega_1 \\ -\omega_3 & 0 & \omega_1 & \omega_2 \\ \omega_2 & -\omega_1 & 0 & \omega_3 \\ -\omega_1 & -\omega_2 & -\omega_3 & 0 \end{bmatrix} \quad (3)$$

and where $\boldsymbol{\omega} = [\omega_1, \omega_2, \omega_3]^T$ is the vector of the roll, pitch and yaw body rates, $\mathbf{q} = [q_1, q_2, q_3, q_4]^T$ is the quaternion vector and $\mathbf{h}_{rw} = [h_{rw1}, h_{rw2}, h_{rw3}, h_{rw4}]^T$ is the vector of the flywheel angular momenta. The principal inertia body-fixed frame is considered, with I_{xx} , I_{yy} , and I_{zz} on the main diagonal of the satellite inertia matrix \mathbf{I}_s .

The considered Attitude Control System (ACS) consists of a fixed array of four reaction wheels in a tetrahedral configuration defined by the matrix \mathbf{T}_{rw} . The elements of the input vector $\mathbf{M} = [M_1, M_2, M_3, M_4]^T$ correspond to the attitude control torques of the reaction wheels.

Equation (1) explicitly includes the gravitational and aerodynamic disturbance torque models \mathbf{M}_{gg} and \mathbf{M}_{aero} about the centre of mass and dependant on the satellite attitude. These disturbances typically represent the most important external disturbance torques affecting Low Earth Orbit (LEO) satellites (Wie (2008)). The design of the FDI system exploits an explicit decoupling only of the aerodynamic torque since the gravitational disturbance has a model which is *almost perfectly known*, and thus it does not need to be decoupled. The gravity gradient torque \mathbf{M}_{gg} is

$$\mathbf{M}_{gg} = \frac{3\mu}{R^3}(\hat{v}_{nadir} \times I_s \hat{v}_{nadir}) \quad (4)$$

where the parameters μ and R represent the gravitational constant and the orbit radius respectively, and \hat{v}_{nadir} is the unit vector towards nadir expressed in body-frame coordinates. The aerodynamic torque \mathbf{M}_{aero} is

$$\mathbf{M}_{aero} = \frac{1}{2}\rho S_p V^2 C_D(\hat{v}_V \times \mathbf{r}_{cp}) \quad (5)$$

where ρ is the atmospheric density, V is the relative velocity of the satellite, S_p is the reference area affected by the aerodynamic flux, and C_D is the drag coefficient. $\mathbf{r}_{cp} = [r_{xcp}, r_{ycp}, r_{zcp}]^T$ is the vector joining the centre of mass and the aerodynamic centre of pressure and \hat{v}_V is the unit velocity vector expressed in body-frame coordinates. It is worth noting that, mainly due to the presence of the unknown terms ρ and C_D in (5), the input \mathbf{M}_{aero} in (1)

represents the main source of uncertainty.

The dynamic equations of the reaction wheel models are

$$\dot{\boldsymbol{\omega}}_{rw} = J_{rw}^{-1}\dot{\mathbf{h}}_{rw} = -J_{rw}^{-1}(\mathbf{M} + b\boldsymbol{\omega}_{rw} + c\text{sgn}(\boldsymbol{\omega}_{rw})) \quad (6)$$

where J_{rw} denotes the flywheel inertia, $\mathbf{h}_{rw} = J_{rw}\boldsymbol{\omega}_{rw}$ is the vector of the flywheel angular momenta, $\boldsymbol{\omega}_{rw} = [\omega_{rw1}, \omega_{rw2}, \omega_{rw3}, \omega_{rw4}]^T$ is the vector of the flywheel spin rates and b , c are the viscous and Coulomb friction coefficients, respectively (Carrara et al. (2012)).

The overall system model is given by (1), (2) and (6). Thus, the overall state vector can be represented by $x = [\omega_1, \omega_2, \omega_3, q_1, q_2, q_3, q_4, \omega_{rw1}, \omega_{rw2}, \omega_{rw3}, \omega_{rw4}]^T$ and all the state variables are assumed to be measurable. Moreover, two different attitude sensors are assumed to be available. The attitude measurements are represented by two different quaternion vectors which are calculated on the basis of the information provided by two physical attitude sensors (*e.g.* star trackers). This hardware redundancy is necessary for the complete fault isolability and comes as outcome of the application of a detectability and isolability study to the proposed fault scenarios.

3. FAULT DETECTION AND ISOLATION

3.1 Actuator and Sensor Fault Modelling

Possible faults affecting the actuated attitude control torques, flywheel spin rate, satellite attitude and angular velocity measurements are considered and it is assumed that at most one fault affects the system at any time.

Since (1) and (6) are affine in the control inputs, the i -th physical actuator fault can be modelled by the following fault input where $M_{c,i}$ is the commanded control input:

$$F_{M_i} = f_{M_i} = M_i - M_{c,i} \quad (i = 1, \dots, 4) \quad (7)$$

The occurrence of sensor faults can be taken into account by defining the faults as the differences between the real values ω_{rwj} , ω_l , q_m and measured values $\omega_{rwj,y}$, $\omega_{y,l}$, $q_{y,m}$:

$$\begin{aligned}F_{\omega_{rwj}} &= \omega_{rwj,y} - \omega_{rwj} & (j = 1, \dots, 4) \\ F_{\omega_l} &= \omega_{y,l} - \omega_l & (l = 1, \dots, 3) \\ F_{q_m} &= q_{y,m} - q_m & (m = 1, \dots, 4)\end{aligned} \quad (8)$$

However, this modelling would lead to the appearance of fault terms in the output equations, or more in general to models nonlinear in the sensor fault inputs.

A different modelling procedure for sensor faults was proposed by Mattone-De Luca (2006) to obtain a dynamic model suitable for the FDI design with a structure affine in all the fault inputs as considered by the NLGA.

Essentially, it consists in introducing a suitable set of $\nu \geq 1$ *mathematical* fault inputs f_k ($k = 1, \dots, \nu$) in place of each *physical* sensor fault F , including also a fault input associated to the time derivative of the fault F . Whenever a physical sensor fault $F \neq 0$ occurs, all the associated mathematical fault inputs f_k will become generically nonzero, although with completely different time behaviors and, in general, without a direct physical interpretation. Hence, it will be sufficient to recognise the occurrence of *any* (one or more) of the associated mathematical fault inputs. For a comprehensive detailed application of this modelling procedure, refer to Mattone-De Luca (2006).

Applying this procedure to (1), (2) and (6), a generic j -th physical flywheel spin rate sensor fault $F_{\omega_{rw_j}}$ ($j = 1, \dots, 4$) can be associated to $\nu_j = 5$ mathematical fault inputs $f_{\omega_{rw_{j,k}}}$ ($k = 1, \dots, \nu_j$). A generic l -th physical satellite angular velocity sensor fault F_{ω_l} ($l = 1, \dots, 3$) can be associated to $\nu_l = 7$ mathematical fault inputs $f_{\omega_{l,k}}$ ($k = 1, \dots, \nu_l$). Physical attitude sensor faults generally affect all the quaternion components simultaneously, thus each sensor fault is thereafter modelled as a single additive fault vector $\mathbf{F}_{\mathbf{q}} = [F_{q_1}, F_{q_2}, F_{q_3}, F_{q_4}]^T$ where each fault vector component F_{q_m} ($m = 1, \dots, 4$) can be associated to $\nu_m = 7$ mathematical fault inputs $f_{q_{m,k}}$ ($k = 1, \dots, \nu_m$). Therefore, if (1), (2) and (6) are rewritten by considering the sensor outputs $\omega_{rw_{y,j}} = \omega_{rw_j} - F_{\omega_{rw_j}}$, $\omega_{y,l} = \omega_l - F_{\omega_l}$, $q_{y,m} = q_m - F_{q_m}$ (*i.e.* $y = x + F_x$) as the new state variables for the system dynamics, the general structure of a nonlinear system for the NLGA, which is affine in both the disturbance (*i.e.* the uncertain aerodynamic force term $d = F_{aero}$), actuator and sensor fault inputs, is recovered:

$$\begin{aligned} \dot{y} = & n(y) + p(y) d_{aero} + \sum_{i=1}^4 g_i(y) M_{c,i} + \\ & + \sum_{i=1}^4 \ell_{M_i}(y) f_{M_i} + \sum_{j=1}^4 \sum_{k=1}^{\nu_j} \ell_{\omega_{rw_{j,k}}}(y) f_{\omega_{rw_{j,k}}} + \\ & + \sum_{l=1}^3 \sum_{k=1}^{\nu_l} \ell_{\omega_{l,k}}(y) f_{\omega_{l,k}} + \sum_{m=1}^4 \sum_{k=1}^{\nu_m} \ell_{q_{m,k}}(y) f_{q_{m,k}} \end{aligned} \quad (9)$$

3.2 Nonlinear Geometric Approach

The NLGA was formally developed by De Persis-Isidori (2001), and it relies on a coordinate change in the state and output spaces providing an observable subsystem which, if it exists, is affected by the fault (or faults) to be detected, but unaffected by any disturbances and the other faults to be decoupled. In the new (local) coordinates, the system can be decomposed into three subsystems \bar{x}_1 , \bar{x}_2 and \bar{x}_3 , where \bar{x}_1 is the measured part of the state affected only by the fault term f to be detected, whilst \bar{x}_2 and \bar{x}_3 represent the measured and not measured part of the state affected by all the faults and disturbances, respectively. For a comprehensive detailed application of the NLGA, refer to De Persis-Isidori (2001) and Baldi et al. (2015). Denoting \bar{x}_2 with \bar{y}_2 and considering it as an independent input, the \bar{x}_1 -subsystem can be defined as follows:

$$\begin{cases} \dot{\bar{x}}_1 = n_1(\bar{x}_1, \bar{y}_2) + g_1(\bar{x}_1, \bar{y}_2) u_c + \ell_1(\bar{x}_1, \bar{y}_2, \bar{x}_3) f \\ \bar{y}_1 = h(\bar{x}_1) \end{cases} \quad (10)$$

with $\ell_1(\bar{x}_1, \bar{y}_2, \bar{x}_3) \neq 0$. Starting from (10), a generic residual generator in filter form is modelled as follows:

$$\begin{cases} \dot{\xi} = n_1(\bar{y}_1, \bar{y}_2) + g_1(\bar{y}_1, \bar{y}_2) u_c + L(\bar{y}_1 - \xi) \\ \varepsilon = \bar{y}_1 - \xi \end{cases} \quad (11)$$

where $L > 0$ is the gain of the asymptotically stable residual filter and ε is the generated diagnostic signal.

3.3 FDI of Actuator and Flywheel Sensor Faults

The NLGA FDI system is designed on the basis of the input affine nonlinear model structure (9) as described in (De Persis-Isidori (2001); Baldi et al. (2015)). Since

the flywheel spin rate measurements are assumed to be available, it is straightforward to design four simple scalar NLGA residual filters independent of the aerodynamic disturbance and satellite attitude and exploiting information provided only by the reaction wheel sensors, directly on the basis of (6). Each of these NLGA residual filters results to be sensitive only to the couple of faults f_{M_i} , $f_{\omega_{w_{j,1}}} = F_{\omega_{w_j}}$ ($i = j$), *i.e.* the actuator and flywheel spin rate sensor faults related to the same i -th reaction wheel, respectively, and the fault input $f_{\omega_{w_{j,5}}} = \dot{F}_{\omega_{w_j}}$, *i.e.* the time derivative of the physical sensor fault. These four filters allow the isolation of the reaction wheel subsystem affected by a possible actuator or flywheel spin rate sensor fault, but not the exact and complete fault isolation. An additional NLGA residual filter is designed to allow the classification of a detected fault. On the basis of (1) and (6), the fifth filter is decoupled from the aerodynamic disturbance, *i.e.* not subject to detection errors due to aerodynamic parameter uncertainties. It exploits all the sensor measurements and it is insensitive to any possible actuator fault and sensitive to all the physical flywheel spin rate sensor faults through the associated mathematical fault inputs. The scalar state variables ξ of the five designed NLGA residual filters are

$$\begin{aligned} \xi_1 &= J_{rw} \omega_{rw_1} / b & \xi_2 &= J_{rw} \omega_{rw_2} / b \\ \xi_3 &= J_{rw} \omega_{rw_3} / b & \xi_4 &= J_{rw} \omega_{rw_4} / b \\ \xi_5 &= r_{x_{cp}} (I_{xx} \omega_1 + \mathbf{T}_1 \mathbf{h}_{rw}) + r_{y_{cp}} (I_{yy} \omega_2 + \mathbf{T}_2 \mathbf{h}_{rw}) + \\ & \quad + r_{z_{cp}} (I_{zz} \omega_3 + \mathbf{T}_3 \mathbf{h}_{rw}) \end{aligned} \quad (12)$$

where \mathbf{T}_1 , \mathbf{T}_2 and \mathbf{T}_3 are the rows of the matrix \mathbf{T}_{rw} .

3.4 FDI of Attitude and Angular Velocity Sensor Faults

Two sets of nine scalar NLGA residual filters organised as *generalised schemes* and decoupled from the aerodynamic disturbance are designed on the basis of (2). Each set exploits the same residual filter models and the same shared angular velocity measurements, but the measurements of a different attitude sensor. Thanks to the NLGA, each of these residual filters results to be sensitive only to a couple of physical angular velocity sensor faults F_{ω_j} and to only one physical attitude sensor fault $\mathbf{F}_{\mathbf{q}_n}$ ($n = 1, 2$) through the associated mathematical fault inputs. The scalar state variables ξ of the nine designed NLGA residual filters are

$$\begin{aligned} \xi_{6,n} &= 1 - 2q_{2,n}^2 - 2q_{3,n}^2 \\ \xi_{7,n} &= 1 - 2q_{1,n}^2 - 2q_{3,n}^2 \\ \xi_{8,n} &= 1 - 2q_{1,n}^2 - 2q_{2,n}^2 \\ \xi_{9,n} &= 2(q_{1,n}q_{2,n} + q_{3,n}q_{4,n}) & \xi_{12,n} &= 2(q_{1,n}q_{2,n} - q_{3,n}q_{4,n}) \\ \xi_{10,n} &= 2(q_{1,n}q_{3,n} + q_{2,n}q_{4,n}) & \xi_{13,n} &= 2(q_{1,n}q_{3,n} - q_{2,n}q_{4,n}) \\ \xi_{11,n} &= 2(q_{1,n}q_{4,n} + q_{2,n}q_{3,n}) & \xi_{14,n} &= 2(q_{2,1}q_{3,1} - q_{1,1}q_{4,1}) \end{aligned} \quad (13)$$

where $\mathbf{q}_n = [q_{1,n}, q_{2,n}, q_{3,n}, q_{4,n}]^T$ ($n = 1, 2$) are the quaternion vectors of the two available attitude sensors.

3.5 Residual Cross-check Scheme for FDI

Assuming a single fault at any time, possible faults affecting the actuated torques or the flywheel spin rate measurements can be detected and isolated by cross-checking the five residuals $\epsilon_1, \dots, \epsilon_5$ of the NLGA filters exploiting the variables (12) described in Section 3.3, as follows:

- (1) Firstly, the first four residuals, which are sensitive only to possible actuator and sensor faults affecting a

specific reaction wheel, are analyzed. Thus, the faulty actuator subsystem can be detected and isolated.

- (2) Then, the fifth residual, which is sensitive only to sensor faults and insensitive to actuator faults, is checked to precisely recognise the occurred fault type.

On the other hand, possible faults affecting the satellite angular velocity or attitude measurements can be detected and isolated by cross-checking the two sets of nine residuals $\epsilon_{6,n}, \dots, \epsilon_{14,n}$, ($n = 1, 2$) of the NLGA filters exploiting the variables (13) described in Section 3.4, as follows:

- (1) Firstly, the two sets are compared. Since each set exploits the measurements of a different attitude sensor and of the same angular velocity sensors, the two sets show different residual behaviours in case of attitude sensor faults and the same residual behaviours in case of angular velocity sensor faults.
- (2) A faulty attitude sensor is isolated by checking which is the only set with signals exceeding the selected thresholds. A faulty angular velocity sensor is isolated by checking the three residuals of each set not sensitive to each possible angular velocity sensor faults.

Finally, due to the presence of measurement noise, residual thresholds have to be properly selected to achieve the best false alarm rate and missed fault rate performances.

4. FAULT DIAGNOSIS

4.1 Radial Basis Function Neural Network

As stated in (Chen-Chen (1995); Castaldi et al. (2014)), for a sufficiently large number N of hidden-layers neurons and if the system state x takes on values in a compact set $X \subset \mathcal{R}^{\ell_n}$, a weight matrix W can be determined such that a generic continuous function $f(x)$ can be approximated by RBFs, with a guaranteed finite model error e^* :

$$f(x) = W\varphi(x) + e(x) = \sum_{k=1}^N w_k \varphi_k(x) + e(x) \quad (14)$$

where W is an *optimal* weight matrix, φ_k is k -th radial basis function and $e(x)$ is the model approximation error satisfying $|e(x)| \leq e^*$. In this paper, the RBFs are assumed to be modelled as Gaussian functions as follows:

$$\varphi_k(\hat{x}) = \exp(-|\hat{x} - \mu_k|^2 / \sigma_k^2) \quad (15)$$

where μ_k and σ_k are the center and the width of the k -th radial basis function, respectively.

4.2 Estimation of Actuator and Sensor Faults

Considering the occurrence of possible actuator torque faults, the model (11) of each of the first four NLGA residual filters described in Section 3.3 is modified, in order to design just as many independent RBF NN adaptive filters to accurately estimate an occurred fault, as follows:

$$\begin{cases} \dot{\xi} = n_1(\bar{y}_1, \bar{y}_2) + g_1(\bar{y}_1, \bar{y}_2) u_c + \\ \quad + \ell_1(\bar{y}_1, \bar{y}_2) f + L(\bar{y}_1 - \xi) \\ \varepsilon = \bar{y}_1 - \xi \end{cases} \quad (16)$$

where the actuator torque fault function $f = F_{M_i}$ ($i = 1, \dots, 3$) is estimated by a RBF NN:

$$\hat{f} = \hat{F}_{M_i} = \hat{W}\varphi(\xi) \quad (17)$$

with the following adaptive law for the weight matrix \hat{W} :

$$\dot{\hat{W}} = \eta D \varepsilon \varphi^T(\xi) \quad (18)$$

where $\eta > 0$ is the learning ratio and D is a proper constant matrix such that (16) is asymptotically stable.

Considering the occurrence of possible flywheel spin rate sensor faults, the model (11) of each of the first four NLGA residual filters described in Section 3.3 is modified in the same way as (16), in order to design just as many independent RBF NN adaptive filters to accurately estimate the combined mathematical sensor fault function $f = -bF_{\omega_{w_j}}/J_{rw} - \dot{F}_{\omega_{w_j}}$ ($j = 1, \dots, 4$):

$$\hat{f} = \hat{W}\varphi(\xi) \quad (19)$$

with the same adaptive law (18) for the weight matrix \hat{W} . Subsequently, the obtained combined fault estimate $\hat{f} = -b\hat{F}_{\omega_{w_j}}/J_{rw} - \hat{F}_{\omega_{w_j}}$ is filtered by means of the first order transfer function $-1/(s + b/J_{rw})$ to estimate the actual physical sensor fault $F_{\omega_{w_j}}$.

Considering the occurrence of possible satellite angular velocity sensor faults, four different scalar residual filters can be designed directly from the equations of (2). Then, the model (11) of each of these new four residual filters can be modified in the same way as (16) and each derived independent RBF NN adaptive filter estimates a different associated mathematical fault inputs $f_{\omega_{l,k}}$ ($k = 4, \dots, 7$):

$$\hat{f} = \hat{f}_{\omega_{l,k}} = \hat{W}\varphi(\xi) \quad (20)$$

with the same adaptive law (18) for the weight matrix \hat{W} . Then, the estimate of the actual physical sensor fault can be derived by exploiting the expressions of the associated mathematical fault inputs $f_{\omega_{l,k}}$.

Finally, considering the occurrence of possible satellite attitude sensor faults, four independent RBF NN adaptive filters and the measurements of the isolated faulty attitude sensor are used to estimate different combinations f_m ($m = 1, \dots, 4$) of mathematical fault inputs associated to the components F_{q_m} ($m = 1, \dots, 4$) of the physical fault:

$$\hat{f} = \hat{f}_m = \hat{W}\varphi(\xi) \quad (21)$$

with the same adaptive law (18) for the weight matrix \hat{W} and with f_m ($m = 1, \dots, 4$) defined as follows:

$$\begin{aligned} f_1 &= (\omega_1 F_{q_4} - \omega_2 F_{q_3} + \omega_3 F_{q_2})/2 - \dot{F}_{q_1} \\ f_2 &= (\omega_1 F_{q_3} + \omega_2 F_{q_4} - \omega_3 F_{q_1})/2 - \dot{F}_{q_2} \\ f_3 &= (-\omega_1 F_{q_2} + \omega_2 F_{q_1} + \omega_3 F_{q_4})/2 - \dot{F}_{q_3} \\ f_4 &= (-\omega_1 F_{q_1} - \omega_2 F_{q_2} - \omega_3 F_{q_3})/2 - \dot{F}_{q_4} \end{aligned} \quad (22)$$

Then, the estimate of the additive fault vector affecting the measured quaternion vector is obtained by exploiting a state observer, where the state consists of the components F_{q_m} ($m = 1, \dots, 4$) of the attitude fault vector:

$$\dot{\hat{\mathbf{F}}}_q = \frac{1}{2} \mathbf{\Omega} \hat{\mathbf{F}}_q - \hat{\mathbf{f}} + L(\mathbf{F}_{q_v} - \hat{\mathbf{F}}_q) \quad (23)$$

with the matrix $\mathbf{\Omega}(\omega)$ of (3), the observer gain $L > 0$ such that it is asymptotically stable, $\hat{\mathbf{f}} = [\hat{f}_1, \hat{f}_2, \hat{f}_3, \hat{f}_4]^T$ and the measured additive fault vector \mathbf{F}_{q_v} given by the difference between the two available attitude measurements.

5. SIMULATION RESULTS

The satellite body is modelled as a rectangular parallelepiped with dimensions 0.6 x 2 x 7.5 m (depth x width x height), aerodynamic torque displacement vector $\mathbf{r}_{cp} = [0.10, 0.15, -0.35]$ m, drag coefficient $C_D = 2.2$, inertia values $I_{xx} = 330 \text{ kg} \cdot \text{m}^2$, $I_{yy} = 280 \text{ kg} \cdot \text{m}^2$, $I_{zz} = 60 \text{ kg} \cdot \text{m}^2$. A flywheel moment of inertia $J_{rw} = 0.05 \text{ kg} \cdot \text{m}^2$ and initial flywheel spin rate values $\omega_0 = [-300, -300, -300, -300]^T$ rpm for the four reaction wheels are assumed. A circular orbit at an altitude of 350 km, with a null inclination and a low Earth equatorial orbit radius $R = 6728.140$ km, an atmosphere density $\rho = \rho_{max} = 6 \cdot 10^{-11} \text{ kg/m}^3$, an orbital velocity $V = 8187.63 \text{ m/s}$, and the Earth's gravitational constant $\mu = 39.86004418 \cdot 10^{13} \text{ m}^3/\text{s}^2$ is considered.

Assuming a single fault at any time, four additive fault scenarios commencing at $t_{fault} = 10$ s are considered:

- (1) actuator fault: $F_{M_2} = -a_M \omega_{rw_2}$ with a_M passing from zero at $t = 10$ s to $= 0.0005 \text{ Nms}$ at $t = 20$ s;
- (2) flywheel sensor fault: $F_{\omega_{rw_2}} = -a_{\omega_{rw_2}} \omega_{rw_2} + b_{\omega_{rw_2}}$ with $a_{\omega_{rw_2}} = 0.05$, $b_{\omega_{rw_2}} = 0.2094 \text{ rad/s} = 40 \text{ rpm}$;
- (3) angular velocity sensor fault: $F_{\omega_3} = -a_{\omega_3} \omega_3$ with $a_{\omega_3} = 0.05$;
- (4) attitude sensor fault: F_{q_1} additive on the first quaternion measurement, corresponding to a constant bias of $-8.7266 \cdot 10^{-4} \text{ rad}$ on the roll angle measurements.

Sensor noises are modelled by Gaussian processes with zero mean and standard deviations equal to 3 arcsec, 3 arcsec/s and 1 rpm for the attitude expressed in Euler angles, satellite angular velocity and flywheel spin rates, respectively. In case of the actuator fault F_{M_2} , Fig. 1 shows the five diagnostic signals $\epsilon_1, \dots, \epsilon_5$ provided by the NLGA residual filters based on the variables (12) described in Section 3.3. In particular, the residual ϵ_2 is sensitive to the couple of faults F_{M_2} , $F_{\omega_{rw_2}}$, whilst the diagnostic signal ϵ_5 is sensitive only to flywheel sensor faults and decoupled from the aerodynamic disturbance. The selected thresholds are depicted for each residual by means of red lines.

As described in Sections 3.3 and 3.5, each of the first four residuals is sensitive only to actuator and sensor faults possibly occurring on a specific reaction wheel subsystem, thus it is possible to detect and isolate the faulty subsystem just by means of these four residuals. After the isolation of the faulty reaction wheel subsystem, a check on the fifth residual allows to precisely isolate also the type of the occurred fault since this residual is sensitive only to sensor faults and insensitive to actuator faults. It does not exceed the selected thresholds in case of actuator faults.

On the other hand, in case of the flywheel spin rate sensor fault $F_{\omega_{rw_2}}$, Fig. 2 shows that the residual ϵ_2 is sensitive to the occurred fault as in the previous case, but now the diagnostic signal ϵ_5 exceeds the selected threshold after the sensor fault occurrence. Hence, the occurred flywheel sensor fault can be correctly isolated thanks to the different behaviour of the fifth residual.

Faults affecting the satellite angular velocity and attitude sensors can be detected and isolated by exploiting the two sets of nine diagnostic signals $\epsilon_{6,n}, \dots, \epsilon_{14,n}$, ($n = 1, 2$) provided by the NLGA residual filters based on the variables (13) described in Section 3.4. Fig. 3 shows the diagnostic signals provided by the first (left, $n = 1$) and second (right,

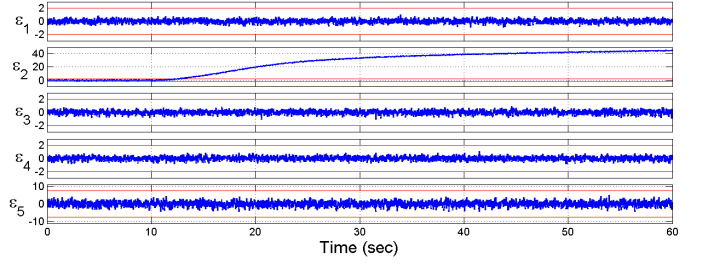


Fig. 1. Actuator fault: four residuals sensitive to faults on a specific reaction wheel and fifth residual sensitive only to flywheel spin rate sensor faults.

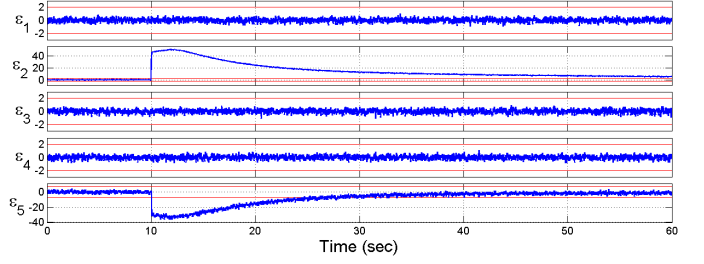


Fig. 2. Flywheel sensor fault: four residuals sensitive to faults on a specific reaction wheel and fifth residual sensitive only to flywheel spin rate sensor faults.

$n = 2$) set of residual filters, which exploits the measurements of the same angular velocity sensors and first and second attitude sensor, respectively. In case of the angular velocity sensor fault F_{ω_3} , both the sets are characterised by the same behaviours. Hence, the occurrence of an angular velocity sensor fault can be detected. In order to isolate the specific faulty sensor, the cross-check of the diagnostic signals of one of the two sets can be performed on the basis of the decision logic described in Section 3.5. In this case, the last three residuals $\epsilon_{8,n}, \epsilon_{10,n}, \epsilon_{14,n}$ of each set are decoupled from possible faults of the third angular velocity sensor and do not exceed their thresholds, in contrast with the other six residuals, which generally are sensitive to the mathematical fault inputs associated to the occurred fault. On the other hand, in case of the attitude sensor fault F_{q_1} , Figs. 4 shows that the two sets are characterised by different behaviours. Hence, the occurrence of a fault affecting the first attitude sensor, which is feeding the set whose residual signals exceed the selected thresholds, can be isolated as described in Section 3.5.

Finally, Fig. 5 shows the fault estimates obtained once the considered faults have been isolated and the proper RBF NN adaptive estimation filters activated. It can be seen that the adaptive filters provide accurate estimates of the occurred faults, even in case of generic fault functions.

6. CONCLUSION

This paper presented a novel scheme for diagnosis of actuator and sensor faults that affect the attitude determination and control system of a low Earth orbit satellite. Despite uncertainties in aerodynamic parameters, fault diagnosis with disturbance decoupling was achieved using a nonlinear geometric approach. The use of radial basis function neural networks was further shown to allow for design of generalised fault estimation filters, able to estimate a generic fault without needing any a priori information

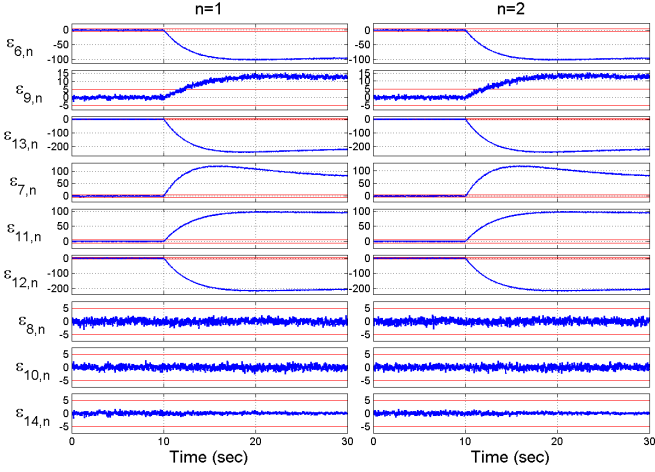


Fig. 3. Angular velocity sensor fault: two sets of nine residuals exploiting the measurements of the first (left, $n = 1$) and second (right, $n = 2$) attitude sensor, respectively.

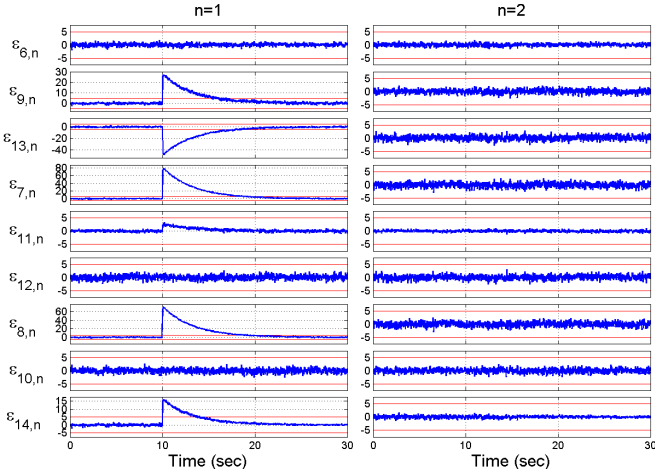


Fig. 4. Attitude sensor fault: two sets of nine residuals exploiting the measurements of the first (left, $n = 1$) and second (right, $n = 2$) attitude sensor, respectively.

about the fault internal model. Simulation results documented the efficacy of the proposed diagnosis scheme to achieve precise fault detection and isolation and provide accurate fault estimates. Further developments will concern the implementation of the proposed scheme in a fault-tolerant control system and a robustness analysis with respect to system parameter uncertainties.

REFERENCES

- Baldi, P., Blanke, M., Castaldi, P., Mimmo, N., and Simani, S. (2015). Combined Geometric and Neural Network Approach to Generic Fault Diagnosis in Satellite Reaction Wheels. *9th IFAC Symposium on Fault Detection, Supervision and Safety for Technical Processes - SAFEPROCESS'15*, Paris (France).
- Blanke, M., Kinnaert, M., Lunze, J., and Staroswiecki, M. (2016). *Diagnosis and Fault-tolerant Control, 3rd Edition*. 3rd edition, Springer-Verlag Berlin Heidelberg.
- Bokor, J. and Szabó, Z. (2009). Fault detection and isolation in nonlinear systems. *Annual Reviews in Control*, 33, 113–123.

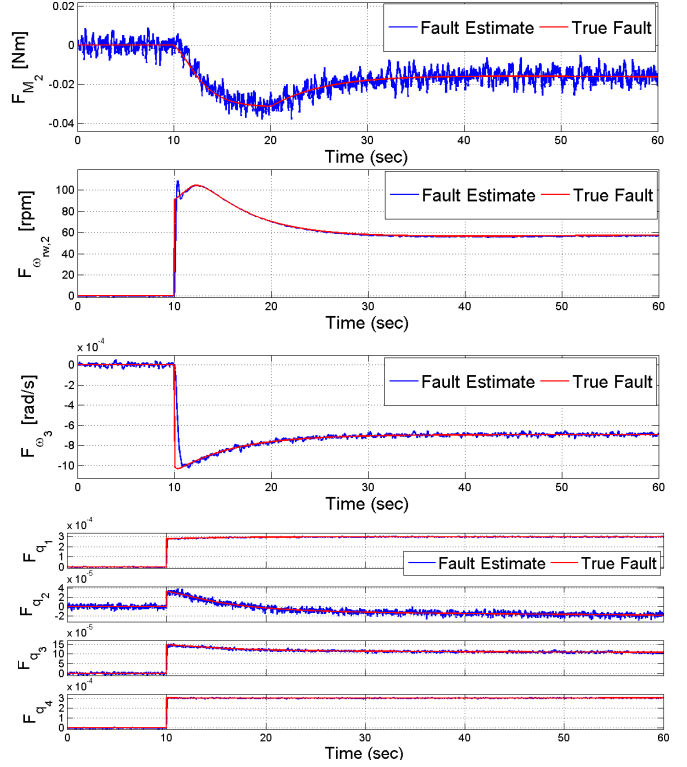


Fig. 5. Estimates of the actuator fault F_{M_2} (a), flywheel sensor fault $F_{\omega_{rw_2}}$ (b), sensor fault F_{ω_3} (c) and additive quaternion fault vector F_{q_1} (d).

- Carrara, V., da Silva, A.G., and Kuga, H.K. (2012). A dynamic friction model for reaction wheels. *1st IAA Conference on Dynamic and Control of Space Systems*, 145, 343–352.
- Castaldi, P., Mimmo, N., Naldi, R. and Marconi, L. (2014). Robust trajectory tracking for underactuated VTOL aerial vehicles: Extended for adaptive disturbance compensation. *Proceedings of the 19th IFAC World Congress, 2014*, 19(1), 3184–3189.
- Chen, T., and Chen, H. (1995). Approximation capability to functions of several variables, nonlinear functionals, and operators by radial basis function neural networks. *IEEE Transactions on Neural Networks*, 6(4), 904–910.
- Chen, J., and Patton, R.J. (1999). *Robust Model-based Fault Diagnosis for Dynamic Systems*. Kluwer Ac. Publ.
- De Persis, C., and Isidori, A. (2001). A geometric approach to nonlinear fault detection and isolation. *IEEE Transactions on Automatic Control*, 45, 853–865.
- Ding, S.X. (2013). *Model-based Fault Diagnosis Techniques: Design Schemes, Algorithms, and Tools*. 2nd edition, Springer-Verlag London.
- Isermann, R. (2011). *Fault Diagnosis Applications: Model-based Condition Monitoring: Actuators, Drives, Machinery, Plants, Sensors, and Fault-tolerant Systems*. Springer-Verlag Berlin Heidelberg.
- Matrone, R., and De Luca, A. (2006). Nonlinear fault detection and isolation in a three-tank heating system. *IEEE Transactions on Control Systems Technology*, 14(6), 1158–1166.
- Wie, B. (2008). *Space Vehicle Dynamics and Control* (2nd ed.). AIAA Education Series.